

Simulationstools II

COMBINING TEMPERATURE AND MASS FLOW AS VARIABLES IN LINEAR OPTIMISATION MODELS

Schönfeldt P.¹, Petrin G.¹, Schlüters S.¹

German Aerospace Center (DLR), Institute of Networked Energy Systems, Oldenburg, Germany, patrik.schoenfeldt@dlr.de, +49 441 99906-465

Abstract

Linear programming is a powerful tool for optimizing unit commitment or power flows in energy supply systems. However, it faces a significant limitation when applied to certain systems. Power in heat supply systems, for example depends on the velocity of the medium as well as temperature. Thus, both quantities must be optimised simultaneously, resulting in a bilinear problem. To address this issue, either of the quantities can be discretised. This paper presents a method that combines the two options by introducing a new heat storage formulation. It also describes mathematical models for heat pumps and solar thermal collectors following the approach.

Keywords

Energy system, Linear programming, Mathematical models, Optimization

1 Introduction

In energy system design, linear optimisation is a commonly used approach. Early studies include the work of Wene [1], who investigated the optimal retrofitting rates for residential buildings in the (that time future) time period between 1980 and 2020. A comprehensive review of current methods can be found in [2].

For heating systems, either temperature of volume flow of the medium is discretised. The present contribution aims to bridge these methods. This way, variables in linear thermal energy system models can be chosen more flexibly, helping to increase the level of detail with a limited increase in computational time. Also, it is possible to easily switch between formulations focused on computational performance and formulations allowing to handle temperatures as variables.

Our description is chosen with an graph based formulation of an energy system in mind that is used in order to formulate a (mixed-integer) linear optimisation problem. In Python, there are several tools implementing that approach, that are often used for expansion planning. For example, there are PyPSA [3], urbs [4], OSeMOSYS [5], FINE [6], PowerGAMA [7], Minpower [8], MOST [9], Calliope [10], and oemof.solph [11]. It is also noteworthy that they have similar dependencies, i.e. most are based on Pyomo [12, 13]. As a result, improvements to one of those tools can generally be adapted for the others. We implemented the method presented in this publication based on *oemof.solph*.

2 Mathematical Problem Description

2.1 Nonlinear Formulation

As a basis, we start with a non-linear formulation. Note that the goal is a mixed-integer linear energy system optimisation model, not an in-detail thermodynamic simulation model. Thus, we already consider quantities as constants where meaningful in the scope of this work. For improved readability, indexes for the components are omitted whenever there is no ambiguity. The indexes i, o

are used to signify input and output.

To optimise energy flows, the most fundamental relation is the one for heat transfer

$$\dot{Q} = \rho c_{\rm p} \dot{V} \times (T_{\rm i} - T_{\rm o}), \tag{1}$$

where ρ is the fluid's density, $c_{\rm p}$ is the heat capacity, \dot{V} describes the (typically variable) volume flow and the T_x describe the temperatures.

2.1.1 Heat Storage

The most simple approach to model heat storage is the fully mixed formulation

$$Q = \rho c_{\rm p} V \times (T_{\rm s} - T_{\rm ref}). \tag{2}$$

It assumes that a volume V has a homogeneous temperature $T_{\rm ref}$. Heat is defined using a reference temperature $T_{\rm ref}$. In particular, temperature distributions and heat flows within the storage tank can be modelled. An example study comparing quadratic modelling approaches using discrete temperatures and discrete volumes to lab measurements is provided by Zinsmeister et al. [14]. As described later also in our present work, the same two options also exist for linear models: Sub-volumes either of variable volume and constant temperature or of constant volume and variable temperature are defined. The fist option can referred to as the moving boundary model, the latter as the nodal model.

2.1.2 Heat Exchanger

The heat exchanger model we use was originally proposed for radiators [15]

$$\dot{Q} = UA \times \frac{(T_{\rm i} - T_{\rm a}) - (T_{\rm o} - T_{\rm a})}{\ln(T_{\rm i} - T_{\rm a}) - \ln(T_{\rm o} - T_{\rm a})},$$
 (3)

where $T_{\rm a}$ is the temperature outside the heat exchanger, A is its surface area, and U is the (assumed to be constant) heat transfer coefficient between the fluid and the

outside. Combination with Eq. (1) yields

$$T_{\rm o} = (T_{\rm i} - T_{\rm a}) \times \exp\left(-\frac{AU}{\rho c_{\rm p} \dot{V}}\right) + T_{\rm a}.$$
 (4)

Note that the formulation is very generic. So not only heat transfer from radiator to a room but also from the soil to a geothermal heat exchanger can be expressed this way. For large areas or small volume flows, the outlet temperature will approach the ambient one, meaning $T_{\rm o} \approx T_{\rm a}$ when the exponential term becomes small.

2.1.3 Solar Thermal Collector

A flat plate solar thermal collector [16, Eq. 6.6.4], can be seen as an extended case of the heat exchanger model as described in Eq. (4). It adds additional contributions by the solar radiation S:

$$\frac{T_{\rm o} - T_{\rm a} - S/U_{\rm L}}{T_{\rm i} - T_{\rm a} - S/U_{\rm L}} = \exp\left(-\frac{U_{\rm L}A_{\rm C}F'}{\rho c_{\rm p}\dot{V}}\right). \tag{5}$$

Here, $U_{\rm L}$ is the heat transfer coefficient from the fluid to the ambient air, $F'=U_{\rm b}/U_{\rm L}$ is the collector efficiency factor, which is constant for given collector design and fluid flow rate, and $A_{\rm C}$ is the collector area. In the collector efficiency factor, $U_{\rm b}=k/L$ is the back loss coefficient (k insulation thermal conductivity).

2.1.4 Heat Pump

Heat pumps are typically modelled based on the theoretical thermodynamic optimum [17], often called Carnot factor

$$\eta_{\rm c} = \frac{1}{COP_{\rm Carnot}} = 1 - \frac{\langle T_{\rm C} \rangle}{\langle T_{\rm H} \rangle},$$
(6)

where

$$\langle T_x \rangle = \frac{T_{x,i} - T_{x,o}}{\ln T_{x,i} - \ln T_{x,o}},\tag{7a}$$

with $x=\mathrm{H}$ signifying the hot and $x=\mathrm{C}$ signifying the cold side connected to the heat pump. For small differences the relation (7a) can be approximated as [17]

$$\langle T_x \rangle \approx \frac{(T_{\rm x,i} + T_{\rm x,o})}{2}.$$
 (7b)

An efficiency factor is then multiplied

$$COP = \eta_{Lorenz} \times COP_{Carnot}$$
 (8)

to obtain realistic values for the COP. Often, $\eta_{\rm Lorenz}$ is set in a way that the characteristics of a specific heat pump are approximated. Using this temperature-dependent factor, energy going in and out of a heat pump can be related using

$$\dot{Q} = P \times COP \tag{9a}$$

$$= \dot{A} \times \left(\frac{COP}{COP - 1}\right),\tag{9b}$$

where \dot{A} is the anergy flow and P is the (typically) electrical power to pump the heat to the higher temperature.

2.2 Linearised Problem Formulation

As seen in Eq. (1), the problem to be solved is of bilinear nature. Because of computational performance, it is advised to linearise the problem [18]. To do so, in our previous work on the topic [19], we decided to discretise the temperatures

$$T_n, n \in \{0, \dots, N-1\},$$
 (10)

leaving \dot{V} to be the optimisation variable. This particularly makes sense when design temperatures are to be met. However, the other choice is possible, thus we define

$$\dot{V}_n, n \in \{0, \dots, N-1\}.$$
 (11)

It is particularly meaningful if part-load operation is avoided anyway, which is the case for many commercially available heat pumps, leaving N=2 to allow either on or off state.

Instead of constraining one component with the temperature of another, it can also be meaningful to define a shared reference temperature. This way, it is possible to express the heat transfer to and from a component separately. The quantities $\dot{Q}_{\rm i}$ and $\dot{Q}_{\rm o}$ can then be calculated using Eq. (1) but using $T_{\rm i}$ or $T_{\rm o}$ as the minuend and $T_{\rm ref}$ as the subtrahend.

2.2.1 Heat Storage

A storage model that works particularly good with discrete temperatures is the moving boundary model, we used in [19]. A more detailed version can be found in [20]. If the temperature is variable, however, fully mixed or nodal storage models are more handy. While use of nodal models in combination with discrete temperature levels for heat production and demand is generally possible and done e.g. in [21], it should be considered that the available temperature depends on the storage content. This way, storage components can be used to switch from discrete temperature to discrete volume or flow component models.

At defined temperature levels, the content of fully mixed heat storage as described by Eq. (2) is

$$Q_n := \rho c_p V \times (T_n - T_{ref}). \tag{12}$$

Now, we want that an active (or usable) level is signified by the binary status variable $y_n(t) \in \{0,1\}$ with

$$y_n(t) = 0 \text{ if } Q(t) < Q_n, \text{ and}$$
 (13a)

$$y_n(t) = 1 \text{ if } Q(t) \ge Q_n. \tag{13b}$$

Note that Q is being optimised, so Eq. (13) cannot be read as a causal relation. We also need a linear formulation. We suggest

$$y_n(t) \le \frac{Q(t)}{Q_n},\tag{14a}$$

$$\hat{y}_n(t) \ge \frac{Q(t) - Q_n}{Q_{\text{max}}},\tag{14b}$$

$$\bar{y}_n(t) = 1 - \hat{y}_n(t),$$
 (14c)

where $Q_{\rm max}$ is the maximum storage content. Equation (14a) guarantees Eq. (13a) but relaxes Eq. (13b) in

the sense that y_n is not forced to be active. To compensate for that, Eq. (14c), enforces $\bar{y}_n=0$ for the given case. The symbol is chosen to emphasise that it can be read as an inverse status. If this should be strictly the case, also

$$1 = y_n(t) + \bar{y}_n(t) \tag{14d}$$

has to be defined to eliminate the possibility that $y_n(t) = \bar{y}_n(t)$, i.e. at $Q = Q_n$, where both can be 1.

Now, note that heat leaving the storage needs to have lower temperature than the storage and higher temperature is needed to increase the storage content. Thus,

$$\dot{Q}_{\text{out},n}(t) \le y_n(t) \times \dot{Q}_{\text{out},\max,n},$$
 (15a)

$$\dot{Q}_{\text{in},n}(t) \le \bar{y}_n(t) \times \dot{Q}_{\text{in,max},n},$$
 (15b)

where $\dot{Q}_{\mathrm{out},n}$ and $\dot{Q}_{\mathrm{in},n}$ denote the heat flow out of and into the storage, respectively, at the temperature T_n . $\dot{Q}_{\mathrm{out,max},n}$ and $\dot{Q}_{\mathrm{in,max},n}$ are the absolute limits of these flows. This way, it is guaranteed that $\dot{Q}_{\mathrm{out}}(t)=0$ if the storage content is not sufficient and $\dot{Q}_{\mathrm{in}}(t)=0$ if the storage content is too high.

So, at each point in time, the storage content Q defines the temperature T in the storage and thus limits the withdrawal temperature or the feed temperature. As multiple output and input flows can be active at the same time, it is meaningful to also define a weighted limit

$$\sum_{n} \dot{Q}_{\text{out},n}(t) \times w(p_n) \le \dot{Q}_{\text{out,max}}, \tag{16}$$

so that the total heat flow out of the storage, and analogously for the input flows, is also constrained.

A further complication comes up due to discrete time steps. If the point in time the storage heat passes a temperature level T_n is not covered by a discrete point in time, $\dot{Q}_{\mathrm{out},n}(t)>0$ will be allowed when the storage temperature is already below T_n on a continuous time scale. This issue can be solved by a time-discrete reformulation of Eq. (15)

$$\dot{Q}_{\text{out},n,t} \le y_{n,t} \times \dot{Q}_{\text{out,max},n},$$
 (17a)

$$\dot{Q}_{\text{in},n,t} \le \bar{y}_{n,t} \times \dot{Q}_{\text{in,max},n},$$
 (17b)

where the index t denotes the time interval between t and $t+\Delta t$. If now the constraint for the status variable is defined by the energy content at the end of that time interval

$$y_{n,t} \le \frac{Q_{t+\Delta t}}{Q_n},\tag{18}$$

it is no longer possible to cross a level T_n using the corresponding power flows. This implies that at any time the lowest level cannot be used for storing energy and energy at the highest level cannot be obtained from the storage. For the extreme case of a fully mixed heat storage, this implication can be read as the fact that a storage will never reach (exactly) the temperature that is used to feed it.

2.2.2 Heat Exchanger

As can be seen in Eq. (4), optimisation of the flow cannot be performed linearly. However, the relation between the temperatures is linear and can be calculated directly if \dot{V} is set. This is particularly interesting when using nodal storage models. When a fully mixed storage model is used as a source, there is no need for optimisation, as the energy will just be drawn from the storage independent from the return temperature.

Still, it is meaningful to define a lower limit for the flow temperature that can still serve the demand. The combination of Eqs. (4) and (1) results in

$$T_{\rm i} = \frac{1}{1 - \exp\left(-\frac{AU}{\rho c_{\rm p} \dot{V}}\right)} \times \frac{\dot{Q}}{\rho c_{\rm p} \dot{V}} + T_{\rm a},\tag{19}$$

which can be used as a lower limit for the storage temperature using the maximum flow for \dot{V} .

2.2.3 Solar Thermal Collector

For discrete temperature levels, possible heat gains can be calculated for every T_n . See [19] for reference. With variable temperature, it is possible to implement Eq. (5) to the linear optimisation. Assuming that the fluid for the collector is directly withdrawn from the storage with a constant flow \dot{V} , the heat drawn from the collector can be expressed as

$$\dot{Q}_{\mathrm{ST,raw}} = \tilde{U}_{\mathrm{C}} \times A_{\mathrm{C}} \times \left(T_{\mathrm{A}} + \frac{S}{U_{\mathrm{L}}} - T_{\mathrm{S}} \right),$$
 (20)

where

$$\tilde{U}_{\rm C} := \frac{\rho c_{\rm p} \dot{V}}{A_{\rm C}} \times \left(1 - \exp\left(-\frac{U_{\rm L} A_{\rm C} F'}{\rho c_{\rm p} \dot{V}} \right) \right)$$
 (21)

is a virtual thermal transmittance. Note that $\dot{Q}_{\rm ST,raw}$ becomes negative for low solar radiation S. Because of this, it is meaningful to restrict the use of the solar collector to times where positive yields can be expected. To include edge cases in the optimisation, a binary variable $y_{\rm ST}$ can be introduced so that the controlled gain is

$$\dot{Q}_{\mathrm{ST}} \leq \dot{Q}_{\mathrm{ST,max}} \times y_{\mathrm{ST}}$$
 and (22a)

$$\dot{Q}_{\mathrm{ST}} \le \dot{Q}_{\mathrm{ST,raw}} + (1 - y_{\mathrm{ST}}) \times \dot{Q}_{\mathrm{ST,max}}.$$
 (22b)

2.2.4 Heat Pump

If temperatures are known a-priory, Eq. (9) can be directly implemented, resulting in a constant COP. This can be considered the standard way to go and is applied e.g. in [22, 23, 24]. In mixed integer models, it is also possible to model part-load efficiencies [25, 18].

If the modelled real-world device does not run in part load, \dot{V} has to be set to the maximum value when the heat pump is running. For other heat-pumps, it can be considered an approximation. Further, it is possible to define a fixed intermediate temperature $T_{\rm M}$ and split the calculation of the performance of the heat pump into two parts. While due to the last term in

$$\varepsilon_{\rm CH} = \varepsilon_{\rm CM} + \varepsilon_{\rm MH} - \varepsilon_{\rm CM} \varepsilon_{\rm MH},$$
 (23)

the total thermodynamic performance is still bilinear, the individual steps just rely on $\varepsilon_{\rm CM}$ and $\varepsilon_{\rm MH}$. In this case, it is a good choice to set the electric power to be discrete. Introducing the binary status variable $y_{\rm HP}$ in Eq. (9) yields

$$\dot{Q} = y_{\rm HP} \times COP \times P \tag{24a}$$

and

$$\dot{A} = y_{\rm HP} \times (COP - 1) \times P. \tag{24b}$$

From these equations in the form $x_b = y \times x$, with a binary variable y, a continuous variable x, and a continuous or zero variable x_b , MILP constraints can be formulated by replacing using [26]

$$x_{\rm b} \le y \times x_{\rm max},$$
 (25a)

$$x_{\rm b} \le x,$$
 (25b)

and

$$x_{\rm b} \ge x - (1 - y) \times x_{\rm max}. \tag{25c}$$

If a linear approximation for the COP is used instead of Eq. (6), both, the higher and the lower temperature can be optimised.

Instead of approximating the COP calculation, also the flow and return temperatures for the warm side can be set. This way, \dot{Q} becomes the defining property of the heat pump model. In that case, Equation (6) can be directly applied and $\langle T_{\rm C} \rangle$ is the variable in a linear equation. In that case, only the approximation of Eq. (7b) has to be used, to replace the mean logarithmic temperature difference by a linear equation. So,

$$\dot{Q} \le \dot{Q}_{\text{max}} \times y_{\text{HP}},$$
 (26a)

meaning that only full-load or no operation is now allowed by the binary status variable $y_{\rm HP}$. Energy conversion

$$\dot{A} = \dot{Q} - P,\tag{26b}$$

allows the use of additional electricity if the cold side cannot provide sufficient anergy. On the other hand, the maximum technical efficiency

$$P \ge rac{\dot{Q}_{
m max}}{\eta_{
m Lorenz}} imes \left(y_{
m HP} - rac{T_{
m C,i} + T_{
m C,o}}{2 imes \langle T_{
m H}
angle}
ight),$$
 (26c)

can be optimised by adjusting the source temperature.

3 Case study

3.1 Energy system layout

The energy system layout is displayed in Fig. 1. Additionally to the components present in oemof.solph, we manually formulated constraints using Pyomo. Its core consists of cold and warm storage tank, $50\,\mathrm{m}^3$ each, that are connected by a heat pump (HP) with $\dot{Q}_{\mathrm{max}} = 250\,\mathrm{kW}$. The heat pump takes heat from the cold storage, rises the temperature and feeds into the warm storage. Both of these storage tanks are modelled to be fully mixed, i.e. their heat content is described by one temperature. A solar thermal collector (ST) with a surface of $500\,\mathrm{m}^2$, flow rate of $21/\mathrm{s}$, efficiency F' = 0.988, and heat loss coefficient of $U_{\mathrm{L}} = 3.5\,\mathrm{W/m}^2\mathrm{K}$ is also connected to both of

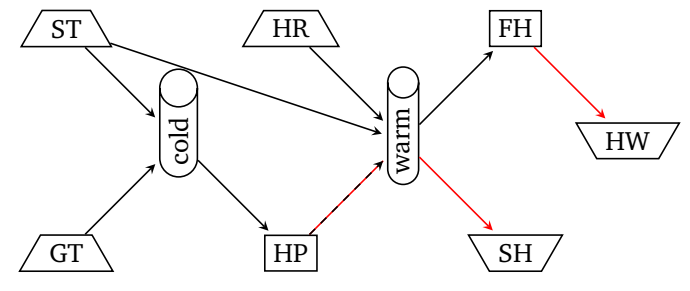


Figure 1: Layout of the energy system graph; the abbreviatiosn stand for ST: solar thermal, HR: heating rod, FH: flow heater, HW: hot water, SH: space heating, HP: heat pump, and GT: geothermal. Arrows point into the direction of heat transfer. Black flows have a variable temperature, red ones a fixed one. The temperatures of heat transfer between heat pump and warm storage are fixed for this study but can be variable using a linear approximation for the COP.

these storage tanks. It can feed either into the cold storage or warm one. The cold storage can also be fed by a geothermal heat exchanger (GT). Its mass flow is fixed so that it delivers $150\,\mathrm{kW}$ at a design $\Delta T = 5\,\mathrm{K}$. We assume that it delivers an outlet temperature which is equal to the soil temperature. Thus, even at constant mass flow, its power will approach zero if cold storage temperature approaches the soil temperature. For warmer storage temperatures, which can be reached using the solar thermal collector, the geothermal heat exchanger is switched off.

So far, the described layout (not the mathematical model of the components) equals the one presented in [19]. However, due to the conceptual difference, two adjustments were made. First of all, our present study does not consider pumping energy needed to fulfil the heat demand. This is in particular due to the choice to set a time-dependent lower temperature limit as defined by Eq. (19), that can still supply the space heating demand (SH) at maximum flow. In the formulation using discrete temperature levels, it was possible optimise the electricity demand of the pumps in a linearised formulation. Secondly, in [19] the temperature of the heat supplied by the heating rod could always be preserved. Due to the fully mixed storage model used in this study, this is no longer the case. While direct electric heating is already part of the heat pump model as described in Eq. (26c), the heating rod is preserved to cover edge cases in the demand where the heat pumps output is not sufficient. The newly added electric flow heater (FH) enables supply of hot water (HW) independently from storage temperature.

3.2 Optimisation results

We performed an economic optimisation where the only considered cost is due to the consumption of electricity by the heat pump and by the flow heater. To facilitate comparability to [19], the same prices based on 2017 day ahead prices where used. Including taxes and levies, they are in the range $34.07 \in /MWh$ to $280.65 \in /MWh$. Example results of the optimisation are displayed in Fig. 2.

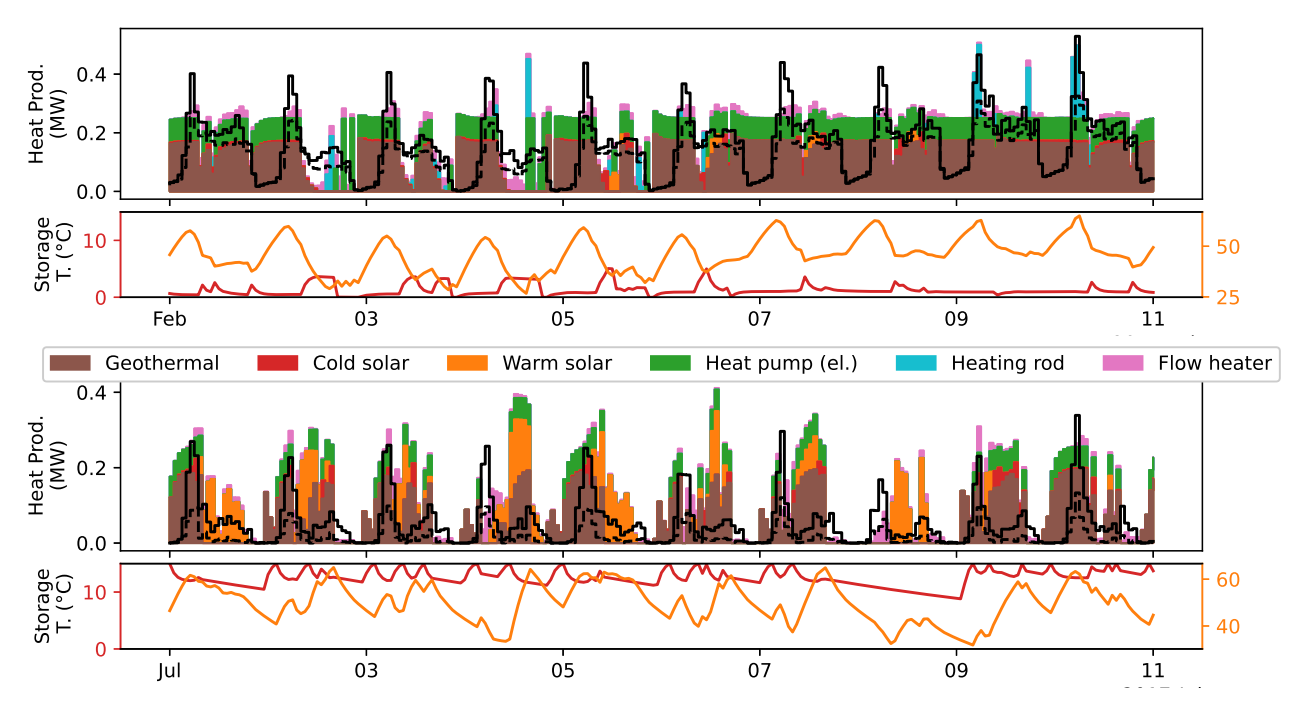


Figure 2: Optimised operation for the energy system for ten days in February (top) and in July (bottom). Coloured areas represent use of the respective heat sources in the time period, the solid black line represents the total heat demand, the dashed black line give the space heating demand. For the storage temperature, the red line represents the cold storage temperature (left axis) and the orange line the warm storage temperature (right axis).

In first ten days of February, a clear preference for geothermal based heating becomes apparent, as a near constant high energy influx in combination with the utilisation of the heat pump can be noticed. Thus the storage temperature of the cold storage is kept low throughout the time frame, to allow for a sufficient amount of geothermal energy extraction. These low temperatures not only benefit the geothermal well, but also the solar thermal collectors, which predominately feed into the cold storage except for day 6-8, where the amount of direct sunlight is sufficient to provide energy to the warm storage. Another noteworthy effect is the low amount of energy from the solar thermal collectors, which enters the cold storage even at night if the outside temperature is above the one of the storage. While the cold storage features no apparent pattern, the hot storage's temperature is closely connected to the demand in space heading and hot water consumption, with temperatures rising before and dropping after the typical morning spike. On the one hand, this reduces the amount of additional heating by the flow heater required for the hot water demand, on the other hand the high up-time of the heat pump, especially near the end of the simulation, indicates that this rise in temperature is also needed as an energy buffer to fulfil the demand. This point is reinforced by the deployment of the electric boiler near the end, which supplements the remaining energy sources with up to 250 kW, to meet demand during the morning spike. Throughout the year, the system operation changes alongside the weather conditions, like shown for the beginning of July. The most noticeable change is the lower share of geothermal power in the system and the increased share of solar thermal heat for the warm storage, which covers most of the afternoon and evening consumption in many cases. The higher share of solar thermal input also highlights the models ability to switch between the hot and cold storages, with feed in into the cold storage now being limited to morning, evening and night time. Despite the higher share of solar thermal, the geothermal well in combination with the heat pump is still crucial to the system, especially during the morning peak or days with lower solar input.

4 Conclusion and Outlook

We have presented a method that allows to optimise temperature as a variable in linear energy system models. The method can be combined with formulations optimising mass flows using discrete temperatures, especially if storage components are present. For those, our presented method can interface with both possible formulations. In a case study using <code>oemof.solph</code>, we have shown a reference optimisation that emphasises the importance of having variable temperatures, e.g. to reduce electricity use of flow heaters or to reduce storage losses between phases of high demand.

For real-world operation, we expect better applicability of operational strategies optimised using variable temperature. This, however, comes at the cost of lower computational performance limiting the applicability of variable temperature methods to shorter time horizons. Average annual metrics like operational costs, on the other hand, should not deviate much, allowing to use discrete temperature methods in the design phase. As adequately

validating the models calls for the transfer of the optimised operational strategies to a real-world device, a comprehensive benchmark of the model, both in terms of computational performance and accuracy, is left for future work.

Acknowledgements

This work has been funded by the German Federal Ministry of Education and Research as part of the Project "Wärmewende Nordwest", Grant No. 03SF0624L.

We thank Lennart Schürmann for discussions about the storage level formulation and Francesco Witte for his idea to introduce a constant intermediate temperature for the heat pump. Maximilian Hillen and Herena Torio are acknowledged for feedback on the manuscript.

References

- [1] C. Wene, "The optimum mix of conservation and substitution: An example from retrofitting of old buildings," *International Journal of Energy Research*, vol. 4, no. 3, p. 271 282, 1980. [Online]. Available: https://onlinelibrary.wiley.com/doi/10.1002/er.4440040309
- [2] M. Hoffmann, B. U. Schyska, J. Bartels, T. Pelser, J. Behrens, M. Wetzel, H. C. Gils, C.-F. Tang, M. Tillmanns, J. Stock, A. Xhonneux, L. Kotzur, A. Praktiknjo, T. Vogt, P. Jochem, J. Linßen, J. M. Weinand, and D. Stolten, "A review of mixed-integer linear formulations for framework-based energy system models," *Advances in Applied Energy*, vol. 16, p. 100190, 2024. [Online]. Available: https://www.sciencedirect.com/science/article/pii/S2666792424000283
- [3] T. Brown, J. Hörsch, and D. Schlachtberger, "PyPSA: Python for power system analysis," *Journal of Open Research Software*, vol. 6, no. 1, p. 4, jan 2018. [Online]. Available: https://openresearchsoftware.metajnl.com/article/10.5334/jors.188/
- [4] J. Dorfner, K. Schönleber, M. Dorfner, sonercandas, froehlie, smuellr, dogauzrek, WYAUDI, Leonhard-B, lodersky, yunusozsahin, adeeljsid, T. Zipperle, S. Herzog, kais siala, and O. Akca, "tum-ens/urbs: urbs v1.0.1," Jul. 2019. [Online]. Available: https://zenodo.org/records/3265960
- [5] M. Howells, H. Rogner, N. Strachan, C. Heaps, H. Huntington, S. Kypreos, A. Hughes, S. Silveira, J. DeCarolis, M. Bazillian, and A. Roehrl, "Osemosys: The open source energy modeling system: An introduction to its ethos, structure and development," *Energy Policy*, vol. 39, no. 10, pp. 5850–5870, 2011, sustainability of biofuels. [Online]. Available: https://www.sciencedirect.com/science/article/pii/S0301421511004897
- [6] L. Welder, D. Ryberg, L. Kotzur, T. Grube, M. Robinius, and D. Stolten, "Spatio-temporal optimization of a future energy system for

- power-to-hydrogen applications in germany," *Energy*, vol. 158, pp. 1130–1149, 2018. [Online]. Available: https://www.sciencedirect.com/science/article/pii/S036054421830879X
- [7] H. G. Svendsen and O. C. Spro, "Powergama: A new simplified modelling approach for analyses of large interconnected power systems, applied to a 2030 western mediterranean case study," *Journal of Renewable and Sustainable Energy*, vol. 8, no. 5, p. 055501, 2016. [Online]. Available: https://doi.org/10.1063/1.4962415
- [8] A. Greenhall, R. Christie, and J.-P. Watson, "Minpower: A power systems optimization toolkit," in 2012 IEEE Power and Energy Society General Meeting, 2012, pp. 1–6. [Online]. Available: https://doi.org/10.1109/PESGM.2012.6344667
- [9] C. E. Murillo-Sánchez, R. D. Zimmerman, C. L. Anderson, and R. J. Thomas, "Secure planning and operations of systems with stochastic sources, energy storage, and active demand," *IEEE Transactions on Smart Grid*, vol. 4, no. 4, pp. 2220–2229, 2013. [Online]. Available: https://doi.org/10.1109/TSG.2013.2281001
- [10] S. Pfenninger and B. Pickering, "Calliope: a multi-scale energy systems modelling framework," *Journal of Open Source Software*, vol. 3, no. 29, p. 825, 2018. [Online]. Available: https://doi.org/10.21105/joss.00825
- [11] U. Krien, P. Schönfeldt, J. Launer, S. Hilpert, C. Kaldemeyer, and G. Pleßmann, "oemof.solph a model generator for linear and mixed-integer linear optimisation of energy systems," *Software Impacts*, vol. 6, Nov 2020. [Online]. Available: https://doi.org/10.1016/j.simpa.2020.100028
- [12] M. L. Bynum, G. A. Hackebeil, W. E. Hart, C. D. Laird, B. L. Nicholson, J. D. Siirola, J.-P. Watson, and D. L. Woodruff, *Pyomo optimization modeling in python*, 3rd ed. Springer Science & Business Media, 2021, vol. 67.
- [13] W. E. Hart, J.-P. Watson, and D. L. Woodruff, "Pyomo: modeling and solving mathematical programs in python," *Mathematical Programming Computation*, vol. 3, no. 3, pp. 219–260, 2011.
- [14] D. Zinsmeister, P. Tzscheutschler, V. S. Perić, and C. Goebel, "Stratified thermal energy storage model with constant layer volume for predictive control formulation, comparison, and empirical validation," *Renewable Energy*, vol. 219, p. 119511, 2023. [Online]. Available: https://www.sciencedirect.com/science/article/pii/S096014812301426X
- [15] S. P. Grétarsson, P. Valdimarsson, and V. K. Jónsson, "Heat transfer modelling of a plate radiator for district heating applications," *International Journal of Energy Research*, vol. 15, no. 4, pp. 301–315,

- 1991. [Online]. Available: https://onlinelibrary.wiley.com/doi/abs/10.1002/er.4440150406
- [16] J. A. Duffie and W. A. Beckman, *Solar Engineering of Thermal Processes*. John Wiley & Sons, Apr. 2013.
- [17] H. Lorenz, "Die Ermittelung der Grenzwerte der thermodynamischen Energieumwandlung," *Zeitschrift für die gesammte Kälte-Industrie*, vol. 2, pp. 27 32, 1895.
- [18] H. Ahmadisedigh and L. Gosselin, "Combined heating and cooling networks with part-load efficiency curves: Optimization based on energy hub concept," *Applied Energy*, vol. 307, p. 118245, 2022. [Online]. Available: https://www.sciencedirect.com/science/article/pii/S0306261921015087
- [19] P. Schönfeldt, A. Grimm, B. Neupane, H. Torio, P. Duran, P. Klement, B. Hanke, K. v. Maydell, and C. Agert, "Simultaneous optimization of temperature and energy in linear energy system models," in 1st International Workshop on Open Source Modelling and Simulation of Energy Systems (OSMSES), 2022, pp. 1–6. [Online]. Available: https://ieeexplore.ieee.org/document/9768967
- [20] D. Muschick, S. Zlabinger, A. Moser, K. Lichtenegger, and M. Gölles, "A multi-layer model of stratified thermal storage for milp-based energy management systems," *Applied Energy*, vol. 314, p. 118890, 2022. [Online]. Available: https://www.sciencedirect.com/science/article/pii/S0306261922003166
- [21] T. Schütz, R. Streblow, and D. Müller, "A comparison of thermal energy storage models for building energy system optimization," *Energy and Buildings*, vol. 93, pp. 23–31, 2015. [Online]. Available: https://www.sciencedirect.com/science/article/pii/S037877881500136X
- [22] K. Vilén and E. O. Ahlgren, "Linear or mixed integer programming in long-term energy systems modeling a comparative analysis for a local expanding heating system," *Energy*, vol. 283, p. 129056, 2023. [Online]. Available: https://www.sciencedirect.com/science/article/pii/S0360544223024507
- [23] A. Meriläinen, J.-H. Montonen, A. Kosonen, T. Lindh, and J. Ahola, "Cost-optimal dimensioning and operation of a solar pv-bess-heat pump-based on-grid energy system for a nordic climate townhouse," *Energy and Build-ings*, vol. 295, p. 113328, 2023. [Online]. Available: https://www.sciencedirect.com/science/article/pii/S0378778823005583
- [24] E. Georges, B. Cornélusse, D. Ernst, V. Lemort, and S. Mathieu, "Residential heat pump as flexible load for direct control service with parametrized duration and rebound effect," *Applied*

- *Energy*, vol. 187, pp. 140–153, 2017. [Online]. Available: https://www.sciencedirect.com/science/article/pii/S0306261916315975
- [25] H.-H. Niu, Y. Zhao, S.-S. Wei, and Y.-G. Li, "A variable performance parameters temperature–flowrate scheduling model for integrated energy systems," *Energies*, vol. 14, no. 17, 2021. [Online]. Available: https://www.mdpi.com/1996-1073/14/17/5400
- [26] U. Krien, C. Kaldemeyer, S. Günther, P. Schönfeldt, H. Simon, J. Launer, J. Röder, C. Möller, J. Kochems, H. Huyskens, B. Schachler, F. Pl, S. Sayadi, P.-F. Duc, J. Endres, F. Büllesbach, D. Fuhrländer, F. Witte, P. Kassing, E. Zolotarevskaia, S. Berendes, B. Lancien, L. Schürmann, J.-O. Delfs, T. Smalla, J. Wolf, E. Gaudchau, T. Rohrer, and M.-C. Gering, "oemof.solph," Jan. 2024. [Online]. Available: https://zenodo.org/records/10497413